

Introduction

Users of MEG are faced with a vast array of inverse methods that can be used to process their data, yet there are few guidelines available to decide which might be appropriate for a given problem. We attempt to address this question using the ROC. The ROC curve is a plot of the trade-off between the probability of true and false positive detection as a function of a single system or operator parameter. This concept can be applied to MEG inverse solutions by computing the ROC curve for detection of known cortical activation. Here we present an objective framework for the evaluation of localization methods in functional neuroimaging, based on the non-parametric free-response ROC (FROC) approach, a modified version of classical ROC framework which allows identification of multiple true and false positives in each image. We apply this objective evaluation criteria to simulated activity at random locations on the cerebral cortex to compare the performances of some source localization algorithms as a function of the size of the activated regions, the number of activated regions, and the degree of correlation between different sources.

Application of FROC to Neuroimaging

We present two different applications of the FROC method to functional neuroimaging which are convenient to control the true and false positive rates respectively:

Type 1:

- A TP occurs if there is at least one active voxel that intersects with an actual blob. An active voxel that is an actual negative is treated as a FP.
- TPF is defined as the fraction of TPs to the total number of actual blobs and FPpl is the mean number of FPs per image, i.e. the average of the FPs over all images.

Type 2

- Apply Connected Component Analysis to the active voxels and group them into activation blobs and accept an activation blob as a true positive if at least half of its voxels intersect with an actual blob or if it includes a large fraction of an actual blob (i.e. $\geq 1/2$) and its size is sufficiently small (e.g. 3 times that of the actual blob) to provide clinically acceptable localization accuracy.
- Accept an activation blob as a false positive if it is not a true positive.

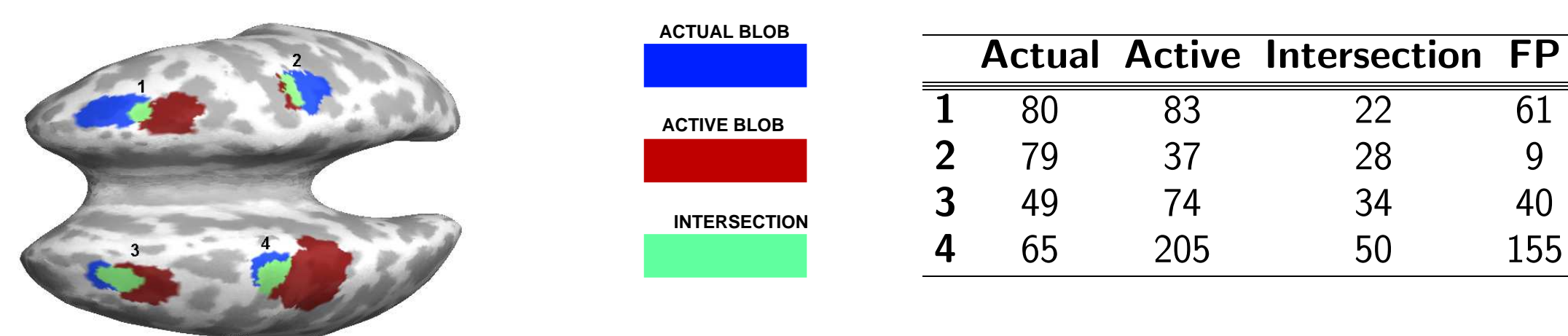


Figure 1: Sample detection map. According to Type1 TPF = 4/4 and FP = 265 whereas according to Type 2 TPF = 2/4 (Blobs 2 & 3 are accepted as true) and FP = 2

Inverse Methods

We give a brief overview of several source localization algorithms whose performance we compare using the FROC.

Regularized Minimum Norm Solutions

A cortical map is computed by fitting the measured data in a least-squares sense. We use Tikhonov regularization to produce a stable solution with regularization parameter λ . We then normalize the minimum norm map to produce a statistic that gives uniform spatial specificity in the absence of activation. This normalization involves division by the expected output in the absence of activation.

$$\begin{aligned} \mathbf{S} &= (\mathbf{G}^T \mathbf{G} + \lambda \mathbf{I})^{-1} \mathbf{G}^T \mathbf{M} = \mathbf{V} \Sigma^+ \mathbf{U}^T \mathbf{M} = \mathbf{H} \mathbf{M} \\ \hat{\mathbf{S}} &= (\text{diag}\{\mathbf{H} \mathbf{C}_N \mathbf{H}^T\})^{-1/2} \mathbf{H} \mathbf{M} \end{aligned} \quad (1)$$

where \mathbf{M} ($n_{ch} \times n_{time}$) represents the measured magnetic field at each sensor as a function of time, \mathbf{G} ($n_{ch} \times 3n_{src}$) is the forward operator and λ is the Tikhonov regularization parameter. $\mathbf{H} = \mathbf{V} \Sigma^+ \mathbf{U}^T$ is the inverse operator having the singular values, $\sigma'_i = \sigma_i / (\sigma_i^2 + \lambda)$. Finally we obtain the detection map as:

$$d_i = E_t \{ \mathbf{s}_i^2(t) \} \quad (2)$$

where \mathbf{s}_i is the reconstructed time-course for surface element i , i.e. the i^{th} row of $\hat{\mathbf{S}}$ in Eq. 1. To find a good regularization parameter, λ , we applied FROC Type 1 and we chose $\lambda = 10^{-9}$ as that which maximized the area under the FROC curve (AUC).

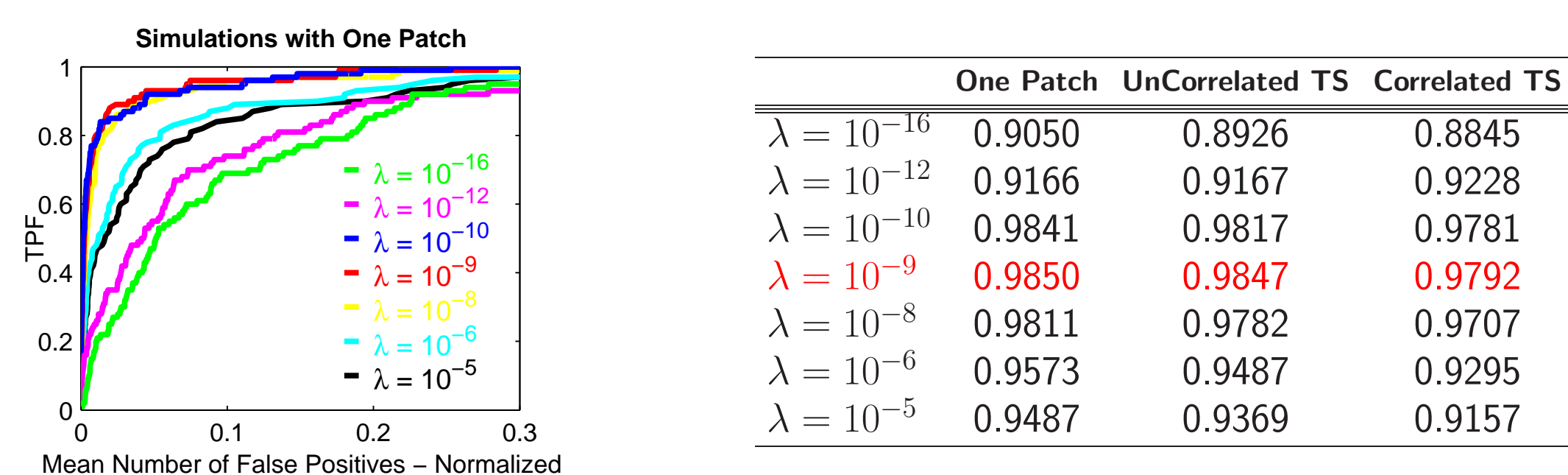


Figure 2: FROC Type 1 curves for different regularization parameters (λ) for simulated images with one patch. Curves are plotted for small values of false positives per image to illustrate differences between the methods. Corresponding AUCs are shown on the right.

Linearly Constrained Minimum Variance Beamformer

LCMV beamformer applies spatial filtering on the sensor array data to discriminate between signals from a location of interest and those originating elsewhere. In application to neuroimaging tasks, the goal is to find a narrow band spatial filter that minimizes the output power of the beamformer subject to a unity gain constraint at the desired location on the brain.

$$\min_{\mathbf{W}_i} \text{tr}\{\mathbf{W}_i^T \mathbf{C}_M \mathbf{W}_i\} \quad \text{subject to} \quad \mathbf{W}_i^T \mathbf{G}_i = \begin{cases} 1 & i=j \\ 0 & i \neq j \end{cases} \quad (3)$$

The LCMV filter weights are given by: $\mathbf{W}_i = [\mathbf{G}_i^T \mathbf{C}_M^{-1} \mathbf{G}_i]^{-1} \mathbf{G}_i^T \mathbf{C}_M^{-1}$, and the neural activity index is defined as the fraction of the estimated signal power over the estimated noise power at location i :

$$d_i = \frac{\text{tr}\{[\mathbf{G}_i^T \mathbf{C}_M^{-1} \mathbf{G}_i]^{-1}\}}{\text{tr}\{[\mathbf{G}_i^T \mathbf{C}_N^{-1} \mathbf{G}_i]^{-1}\}} \quad (4)$$

Multiple Signal Classification (MUSIC)

The MUSIC method identifies sources that maximize the correlation between the signal subspace \mathbf{U}_s and the lead field \mathbf{G}_i . We can generate a cortical detection map, \mathbf{d} as:

$$d_i = \max_{\text{subcorr}}\{\mathbf{G}_i, \mathbf{U}_s\} = \max_{\Sigma_c} \quad \text{where} \quad \mathbf{C} = \mathbf{U}_s^T \mathbf{U}_{dipole} = \mathbf{U}_c \Sigma_c \mathbf{V}_c^T \quad (5)$$

for each spatial location, i .

Matched Filter

A sequence of measurements is compared, or matched, to the expected signal (template), and the filter output indicates the confidence for the existence of the signal. We assume the spatiotemporal channel data are scaled versions of the columns of the forward field:

$$\mathbf{t}_i = \sum_{j \in N_i} c_j \mathbf{g}_j \quad (6)$$

where the set N_i contains voxels in a neighborhood of source i ; for example a 2cm^2 patch. The coefficients c_j scale the activation within the patch, applying more weight near the center of the patch. Then the matched filter output for patch i at time t is given by the sufficient statistic for the source:

$$d_i(t) = \frac{\mathbf{t}_i^T \mathbf{m}(t)}{\sigma \sqrt{\mathbf{t}_i^T \mathbf{t}_i}} \quad (7)$$

The detector output is obtained using the average power of the detection maps; $d_i = E_t \{ d_i^2(t) \}$.

Simulations

A total of 600 MEG datasets were simulated each having 151 MEG sensors, and 300 timepoints. The first 100 datasets represent measurements with no activation on the cortical surface, i.e. white noise on the sensors only. Another 100 datasets represent sensor recordings with one activated patch on the cortical surface. The remaining 400 datasets had two activated patches, and were equally divided into all four combinations of spatially/temporally correlated/unrelated patches. The position of each patch was randomly selected, but restricted on the cortical surface and remained constant over the 300 timepoints.

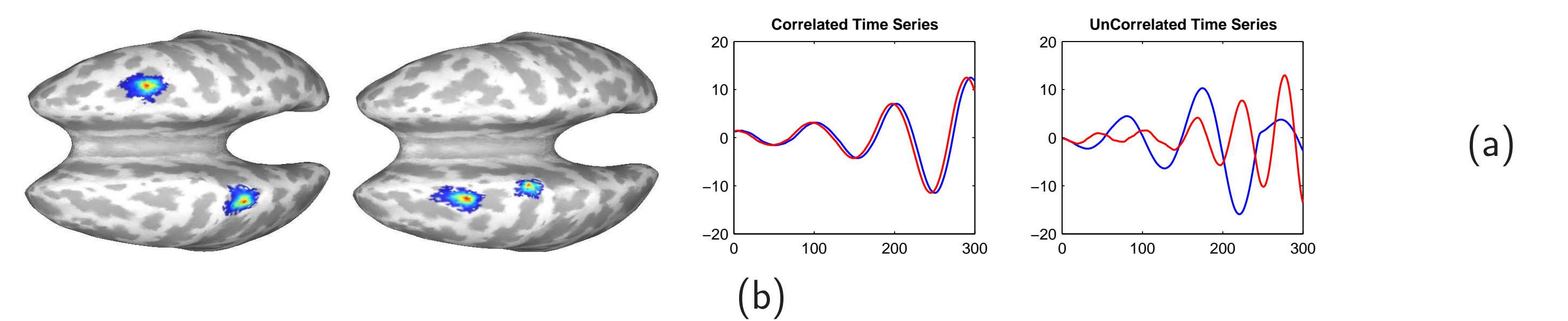


Figure 3: (a) Examples of spatially correlated and uncorrelated simulated sources. SNR is approximately 5. (b) Time Series applied to the simulated MEG data. Correlation coefficients are 95.21% and 5.32% respectively.

Results

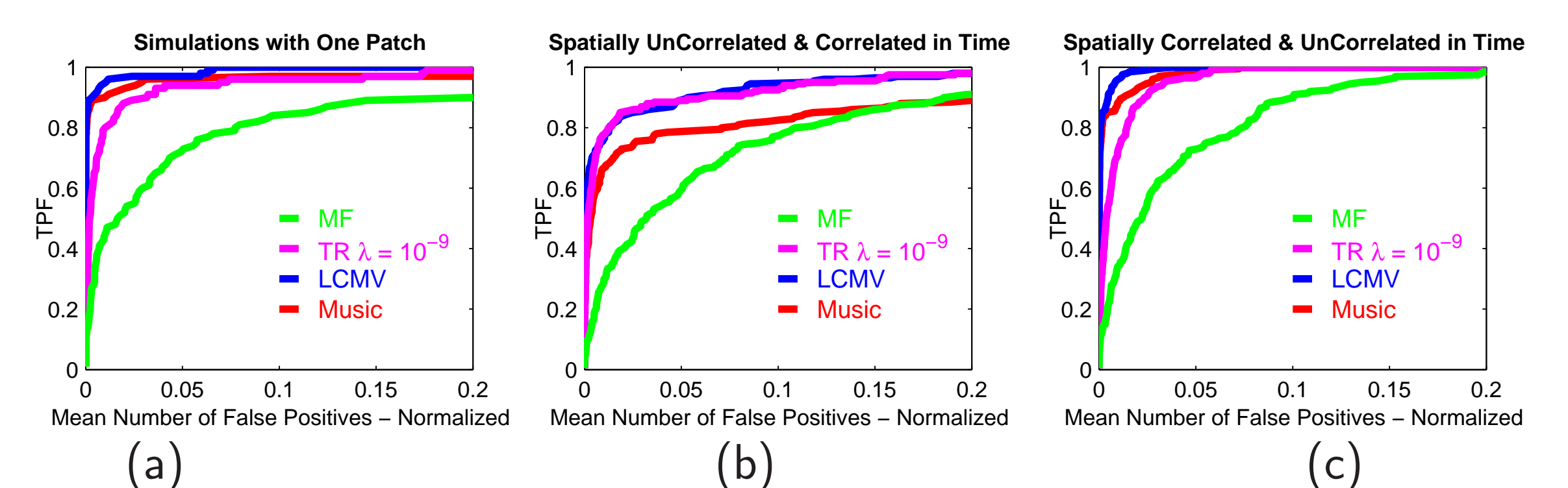


Figure 4: Examples of Application of FROC Type 1. (a) FROC Type 1 Curves for simulated images with 1 patch, (b) for images with two spatially correlated patches having correlated time courses, (c) for images with two spatially uncorrelated patches having uncorrelated time courses.

	AUCs - ONE PATCH		AUCs - TWO PATCHES			
	3cm ²	4cm ²	TC-SC	TC-SU	TU-SC	TU-SU
MUSIC	0.9904	0.9905	0.9840	0.9463	0.9963	0.9897
LCMV	0.9973	0.9974	0.9926	0.9814	0.9986	0.9954
TR $\lambda = 10^{-9}$	0.9859	0.9862	0.9844	0.9843	0.9912	0.9868
MF	0.9471	0.9472	0.9402	0.9310	0.9604	0.9422

The left table shows consistently superior performance of LCMV independent of patch size for a single patch. The right table demonstrates differences depending on the degree of spatial correlation (proximity) and temporal correlation.

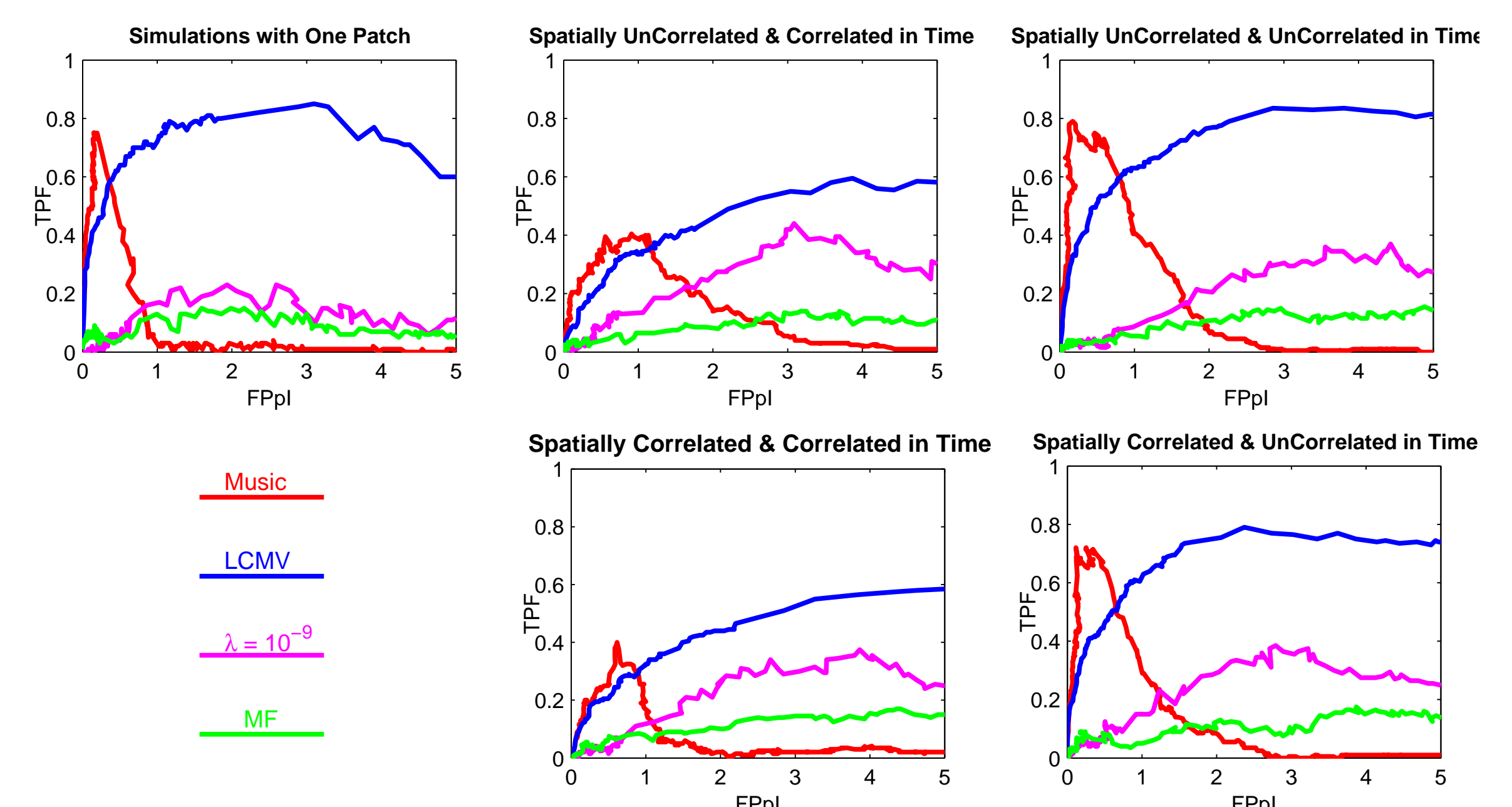


Figure 5: FROC Type 2 Curves for different spatial/temporal correlations. Curves are shown only for $\text{FPpl} \leq 5$ for detailed illustration.

The curves in Fig 5 do not exhibit the standard monotonic behavior of ROC curves. This is because as connected components grow in size we will typically have fewer total blobs, and hence the false positive rate can decrease as the true positive rate increases. However, these plots are interesting since they demonstrate differences in performance not apparent in the Type 1 FROCs in Fig 4. In particular, they demonstrate that, under the type 2 definitions, the MUSIC method achieves its maximum TPF at substantially lower FPpl than the other methods.